# Perturbation of the Izmit earthquake aftershock decaying activity following the 1999 $M_w$ 7.2 Düzce, Turkey, earthquake

Guillaume Daniel,[1] David Marsan,[2] and Michel Bouchon[1]

Received 4 August 2005; revised 9 January 2006; accepted 26 January 2006; published 17 May 2006.

[1] Triggering and quiescence patterns of seismicity in western Turkey, following the occurrence of the 12 November 1999 $M_w$ 7.2 Düzce earthquake are investigated. The changes in seismicity rate are analyzed along the North Anatolian Fault segments that had ruptured 3 months earlier during the 17 August 1999 $M_w$ 7.4 Izmit earthquake. Detection of triggering and quiescence is done by comparing the seismicity rate that would be expected if the Düzce earthquake had not happened to the actual observed rate. The expected rates are estimated by extrapolating the preexisting seismicity pattern, using two complementary models: a simple Omori-Utsu's law and the ETAS model. Fault segments located to the east of the Izmit epicenter show a mild case of quiescence following the Düzce earthquake. These segments had previously experienced an anomalous triggering episode in the 5 days preceding the Düzce earthquake, correlated with the occurrence of two strong ($M_w \geq 5$) Izmit aftershocks. However, it is not clear whether this observed quiescence is real or spurious, as it coincides with a local reconfiguration of the seismological network: a temporary increase of 0.1 to 0.15 in completeness magnitude would be enough to explain this apparent deactivation. Fault segments located to the west of the Izmit epicenter exhibit triggering of seismicity following the Düzce earthquake. This observed triggering is mostly restricted to a cluster of events located in the geothermal area of Yalova. The increase of seismicity rate is delayed by 18 hours after the waves travelling from the Düzce rupture had hit this zone. Our analysis suggests that this 15-day-long reactivation can be explained by a short-lived perturbation, the local seismic activity then sustaining itself for the remaining 15 days. We argue that this particular behavior is likely to correspond to a case of dynamic triggering. By the end of year 1999, the Yalova cluster shows a significant quiescence that lasted for several months; this shutting down does not coincide with the occurrence of any local earthquake that would be large enough to stress shadow this area, suggesting an aseismic cause to this pattern. These results highlight the fact that (1) seismicity triggered by a major earthquake is not restricted to areas loaded by static stress and (2) that seismic activity associated with geothermal geological settings is highly sensitive to stress perturbations, but also to aseismic processes, that can both delay reactivation and cause this activity to suddenly decrease.

**Citation:** Daniel, G., D. Marsan, and M. Bouchon (2006), Perturbation of the Izmit earthquake aftershock decaying activity following the 1999 $M_w$ 7.2 Düzce, Turkey, earthquake, *J. Geophys. Res.*, *111*, B05310, doi:10.1029/2005JB003978.

## 1. Introduction

[2] On 17 August 1999, a $M_w$ 7.4 earthquake occurred on the North Anatolian Fault (NAF), causing more than 18,000 casualties. The epicenter was located near Izmit, Turkey (40°45′N, 29°51.6′E) and the associated rupture extended over 150 km, from the bay of Yalova to the region of Karadere (Figure 1). Three months later, on 12 November 1999, a $M_w$ 7.2 earthquake propagated the rupture 40 km eastward. The epicenter of this second main shock was located in the vicinity of Düzce, Turkey (40°45.6′N, 31°09.6′E).

[3] The NAF is one of the most seismically active region of the world as it experienced 10 $M \geq 7$ events during the 20th century. The most recent strong seismic activity along this fault system is related to the Izmit-Düzce earthquake sequence, which also presents a short interevent time compared to the mean occurrence rate of $M \geq 7$ events during the last century. The proximity and rapid succession of these two events clearly suggests that some interaction mechanism dwelled in the sequence nucleation process. Nevertheless, the nature of this interaction is still prone to discussion. On one hand, static stress calculations based on

[1] Laboratoire de Géophysique Interne et Tectonophysique, Université Joseph Fourier, Grenoble, France.
[2] Laboratoire de Géophysique Interne et Tectonophysique, Université de Savoie, Le Bourget du Lac, France.


0148-0227/06/2005JB003978$09.00

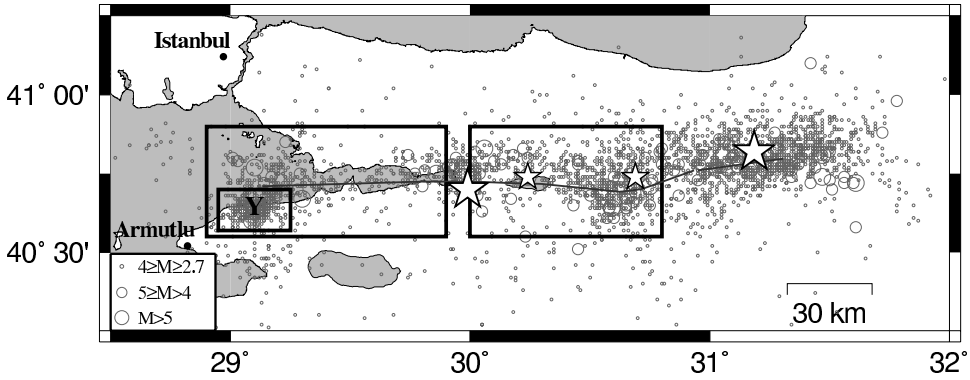


**Figure 1.** Map of northwestern Turkey. Circles stand for all $M \geq 2.7$ events occurring from just after the Izmit earthquake (17 August 1999, day 229) to the end of year 2000. The two large stars indicate Izmit and Düzce epicenters, and the smaller stars show the location of the two $M_w \geq 5$ Izmit aftershocks occurring in the 5 days before the Düzce earthquake. Rectangles delimitate the three areas on which we focused our seismicity analysis. The seismicity swarm located close to Yalova is indicated by the Y. We also locate the city of Armutlu, where well data are available.

historical seismicity provide strong arguments for static triggering by (1) showing that the Izmit earthquake occurred in an area of Coulomb stress increase caused by major earthquakes of the 20th century [*Nalbant et al.*, 1998; *Parsons et al.*, 2000], and (2) highlighting the triggering role of the Izmit event on the Düzce earthquake. Particularly, *King et al.* [2001] and *Utkucu et al.* [2003] reported several bars of Coulomb static stress increase along the Düzce fault following the Izmit earthquake. *King et al.* [2001] also predicted a 1 to 5 bar stress increase in the eastern Marmara Sea, strongly increasing the seismic hazard in Istanbul (12 million inhabitants). On the other hand, postseismic slip inversion and viscous creep modeling, both based on GPS measurements [*Bürgmann et al.*, 2002; *Hearn et al.*, 2002], suggest that the 3 month delay period between these two shocks can be due to a slow loading of the Düzce segment caused by lower crust afterslip on the Karadere segment of the Izmit rupture. This afterslip was estimated to 0.4 m at 25 km depth [*Hearn et al.*, 2002].

[4] A complementary approach validating these mechanical models and providing additional information about the triggering mechanism comes from the analysis of microseismicity. For example, the good correlation between aftershock locations and positive Coulomb static stress lobes [*Stein et al.*, 1992; *King et al.*, 1994] supports the hypothesis that stress redistribution caused by the main shock durably affects the crust and the distribution of aftershocks. However, the existence of stress shadows predicted by the static stress model is still questionable as stress shadows do not systematically show activity rate decreases [*Marsan*, 2003; *Felzer and Brodsky*, 2005], or only develop after a period of reactivation [*Ma et al.*, 2005]. A further step toward the understanding of the triggering mechanism is to propose that transient seismic waves emitted from a main shock are able to cause a sudden increase in seismicity rate, out to distances where the static stresses become negligible. Such phenomenon was observed in the western United States following the 1992 *M* 7.3 Landers, California, earthquake [*Hill et al.*, 1993; *Kilb et al.*, 2000; *Gomberg et al.*, 2001], in Greece following the 1999 *M* 7.4 Izmit, Turkey, earthquake [*Brodsky et al.*, 2000], in western Canada and United States following the 2002 *M* 7.9 Denali, Alaska, earthquake [*Husen et al.*, 2004; *Prejean et al.*, 2004; *Gomberg et al.*, 2004], or at Mount Wrangell, Alaska following the 2004 *M* 9.0 Sumatra earthquake [*West et al.*, 2005].

[5] In this context, the goal of this paper is to study the pattern of triggering/quiescence generated by a strong earthquake, and to confront this observation with existing models. Although there is no obstacle in detecting activation episodes, quiescence is harder to detect when the seismicity level is low prior to an earthquake [see *Marsan and Nalbant*, 2005]. The Izmit-Düzce doublet is therefore of particular interest for studying triggering processes: the pattern of triggering due to the second shock can be well constrained because of the prior high seismicity levels generated by the first shock. It then becomes possible to estimate how the second shock affects the regional seismicity distribution and to characterize the interaction between these two spatially and temporally related large main shocks. This approach was also taken by *Toda and Stein* [2003] and *Woessner et al.* [2004] with the Kagoshima sequence in Japan and by *Marsan and Nalbant* [2005] with the Joshua Tree-Landers sequence.

[6] This study thus focuses on analyzing the seismic response of regional faults previously activated by the Izmit earthquake following the occurrence of the Düzce earthquake. We measure the activations and quiescences in the 3 months following the Düzce event. Finally, we closely examine a cluster of aftershocks located close to the town of Yalova (Figure 1). This cluster, which is characterized by a stronger activity than its surroundings, is clearly affected by the Düzce earthquake, undergoing a reactivation after a delay of several hours following the occurrence of that event.

## 2. Data

[7] We use a catalogue from the Kandilli Observatory and Earthquake Research Institute (Istanbul, Turkey) composed of 5488 events between 17 August 1999 (day 229) and 31 December 2000 (day 731). We consider the catalogue

to be complete for events with magnitude above $M_c = 2.7$, based on the validity of the Gutenberg-Richter law for higher magnitudes. However, we probably miss numerous aftershocks in the first days following the main shocks, leading to an underestimation of hypothetic triggering episodes. Also, there is a 1-day gap in the catalogue between 20 August (day 232) and 21 August 1999. Magnitudes of the events were selected keeping, by order of availability, $M_w$, $M_L$, $M_S$, $m_b$ and $M_D$.

## 3. Method for Measuring Seismicity Triggering and Quiescence

[8] Here we describe the method for measuring changes in seismicity rates following the Düzce earthquake. For a given area, the seismicity rate $\lambda(t)$ prior to the Düzce earthquake is estimated versus time. This estimation is done by fitting a parameterized seismicity model to the observed earthquake occurrence times, for the time interval spanning from the Izmit earthquake at time $T_I$ to just before the Düzce earthquake at time $T_D$. We then compare the observed rate during a given period following the Düzce earthquake to the rate that would be expected if this earthquake had not occurred. In a way, this amounts to "deconvolving" the influence of the Düzce earthquake on the seismicity rate.

[9] Seismicity is modeled as a Poisson stochastic process. The seismic activity in a temporal interval of length $\Delta t$ is seen as the result of a chance process to observe $k$ events due to the activity rate $\lambda(t)$. The probability of occurrence of $k$ events during this time interval is given by

$$P(k|\Lambda) = e^{-\Lambda}\frac{\Lambda^k}{k!} \tag{1}$$

with $\Lambda = \int_t^{t+\Delta t} \lambda(s)\, ds$. As expressed in equation (1), this probabilistic description of seismicity strongly relies on the estimated activity rate $\lambda(t)$. In order to estimate this rate, we use two models: a simple Omori-Utsu's law [*Utsu*, 1961]

$$\lambda(t) = \frac{K}{(t+c)^p} \tag{2}$$

where $t$ denotes the elapsed time since the Izmit earthquake. The parameter set $\theta$ is $\{K, c, p\}$. The second one is the epidemic-type aftershock sequence (ETAS) model [*Ogata*, 1992] with no background seismicity term, which is negligible in the present application:

$$\lambda(t) = \sum_{i;t_i<t} \frac{Ke^{\alpha(m_i-M_c)}}{(t-t_i+c)^p} \tag{3}$$

Here $\theta = \{K, \alpha, c, p\}$. We fit the model to the occurrence times $t_i$ and magnitudes $m_i$ of the earthquakes located in the area that occurred during the time interval $[T_I; T_D]$. This is done using a maximum likelihood inversion technique. In practice, this consists in finding the optimal parameter set $\theta^\star$ that will lead to the minimum of the following cost function [*Ogata*, 1992]:

$$J = \int_{T_I}^{T_D} \lambda(t)dt - \sum_{i;T_I\le t_i<T_D} \ln \lambda(t_i) \tag{4}$$

This model is then extrapolated to the subsequent interval $[T_D + \Delta_1;\ T_D + \Delta_2]$, corresponding to our target period of investigation. In our case, this provides an estimation of the expected rate $\lambda_0$ if the Düzce earthquake had not occurred, based on the Izmit earthquake aftershock sequence up to $T_D$.

[10] We predict this post-Düzce activity rate with no a priori knowledge on the upcoming seismicity using the Omori-Utsu's law:

$$\lambda_0(t \in [T_D+\Delta_1; T_D+\Delta_2]) = \frac{K^\star}{(t+c^\star)^{p^\star}} \tag{5}$$

with the best fitted parameter set $\theta^\star = \{K^\star; c^\star; p^\star\}$ adjusted on the pre-Düzce seismicity. We also extrapolate the pre-Düzce rate with the ETAS model [*Ogata*, 1992]:

$$\lambda_0(t \in [T_D+\Delta_1; T_D+\Delta_2]) = \sum_{i;T_I\le t_i\le T_D+\Delta_2} \frac{K^\star e^{\alpha^\star(m_i-M_c)}}{(t-t_i+c^\star)^{p^\star}} \tag{6}$$

Compared to the extrapolation based on the Omori-Utsu's law, this extrapolation treats the earthquakes occurring after the Düzce event as potential triggers. If the observations depart from this extrapolated rate, then the adjusted model can be considered as not being adapted anymore to the seismogenic process acting in the time interval $[T_D + \Delta_1;\ T_D + \Delta_2]$, i.e., the parameter set $\theta$ characterizing this interval is significantly different from $\theta^\star$.

[11] These two approaches provide complementary measures. Vigorous triggering immediately after the Düzce earthquake will be seen as such (i.e., triggering) by the Omori-Utsu extrapolation, while the ETAS extrapolation can classify this time period as quiescence if the rate of triggered earthquakes after Düzce is too low compared to what the ETAS model had predicted. The latter procedure [*Ogata*, 1992, 1999, 2005] therefore probes changes in the capacity of local earthquakes to trigger one another. It measures changes relative to a "normal" triggering sequence, rather than the absolute level of triggering/quiescence as is done with the Omori-Utsu's law. This is illustrated in Figure 2: an ETAS model is run, starting from the occurrence of a large main shock mimicking the Izmit earthquake. At time $t = 100$, a second large main shock occurs, causing the ETAS parameter $K$ to be halved. Earthquakes then only trigger half of the local seismicity they used to before this second shock. Absolute triggering is observed by the Omori-Utsu extrapolation, while the ETAS extrapolation senses an anomalous dip in activity relative to what this second main shock would have been expected to generate.

[12] This twofold procedure is particularly well suited to test whether seismic activity underwent a short-lived, transient perturbation. Such perturbation would lead to the occurrence of some unexpected aftershocks soon after the perturbation. Subsequently, these would generate their own secondary aftershocks sequence. Seismicity rate of this secondary process is therefore expected to be governed by the same generation process that governed seismicity before the perturbation occurred. In this case, it is predicted that significant triggering is seen by the Omori-Utsu's law, while the ETAS extrapolation does not depart from the observed seismicity rate: the triggered activity can last much longer

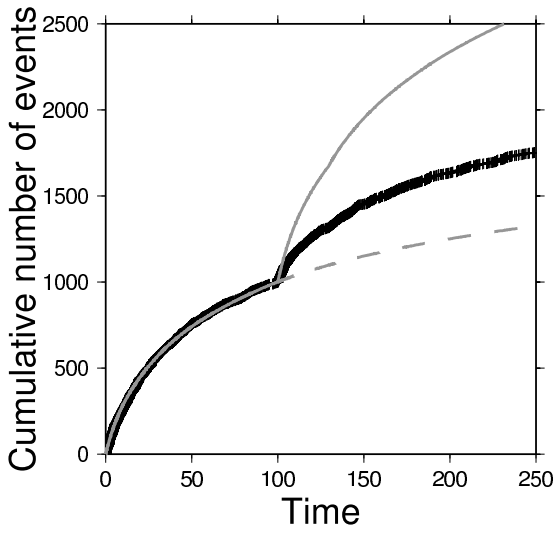


**Figure 2.** Cumulative number of earthquakes (pluses) for a run of an ETAS model, triggered by a large main shock at $t = 0$. A second main shock occurs at $t = 100$, causing the ETAS parameter $K$ to be divided by two. Dashed line indicates extrapolation of the seismicity rates at $t \geq 100$ using an Omori-Utsu's law fitted on the $0 \leq t < 100$ interval, showing clear triggering caused by the second main shock. Solid line indicates extrapolation based on the ETAS model, also fitted on the same $0 \leq t < 100$ interval but uses the earthquakes at $t \geq 100$ as potential triggers. This extrapolation would predict stronger triggering than is observed because of the decrease of parameter $K$ and would thus conclude a relative quiescence.

than the duration of the perturbation because it is self-sustained. This most notably happens when the first few triggered earthquakes have relatively large magnitudes, hence locally triggering their own local aftershock sequences. This procedure thus amounts to deconvolving the triggered seismicity with the local response to a perturbation. Likely causes for triggering seismic activity may either be related to static or dynamic stress transfers.

[13] We also attempted to run a mean-field extrapolation of the ETAS model, which leads to an estimation of the expected activity rate $\lambda_0(t)$ with no a priori knowledge of the post-Düzce seismicity, to double check the results obtained with the Omori-Utsu extrapolation. This is particularly important in zones where the activation caused by the Izmit earthquake is more complex than a simple Omori-Utsu relaxation. However, such mean-field extrapolations systematically lead to unstable and unrealistic activity rate $\lambda_0$, caused by a branching ratio very close to 1; see Appendix A for a thorough development on this. Also, the seismicity time series examined in the present work are all well fit with the Omori-Utsu model; hence a double check was not crucial here.

[14] Finally, we quantify whether the observed number of earthquakes departs significantly from the prediction. To do so, we compare $\lambda_0$ to the probability density function (PDF) of the observed seismicity rate $f_1(\lambda_1)$, expressed as the probability that the $N$ events that were actually observed to occur in the target time interval $[T_D + \Delta_1; T_D + \Delta_2]$ result from a Poisson process with mean $\lambda_1$:

$$f_1(\lambda_1) = e^{-\lambda_1} \frac{{\lambda_1}^N}{N!} \tag{7}$$

We calculate $P$ the probability of triggering as the probability that $\lambda_1 > \lambda_0$ [*Marsan*, 2003]:

$$P = \int_{\lambda_0}^{\infty} f_1(\lambda_1) d\lambda_1 = 1 - \Gamma_i(\lambda_0, N+1) \tag{8}$$

where $\Gamma_i$ stands for the incomplete gamma function. *Marsan* [2003] further defined the $\gamma$ statistics as

$$\gamma = -\mathrm{sgn}(P - 1/2) \log_{10} [\min(P, 1-P)] \tag{9}$$

This, for example, implies that $P = 99.9\%$ corresponds to $\gamma = +3$ or that $P = 0.001\%$ corresponds to $\gamma = -5$. Triggering with 99% significance level therefore implies that $\gamma > 2$, while quiescence with the same significance requires that $\gamma < -2$.

## 4. Changes in Seismic Activity Along the North Anatolian Fault

[15] We run this analysis along the NAF, from longitude 28.9°E to 30.8°E, which corresponds to a part of the fault segments that ruptured during the Izmit earthquake (Figure 1). We could not consider seismicity rate variations to the east of the Karadere segment, due to the spatial limitation of the catalogue used (containing aftershocks located up to only 32°E) and to the very low seismic activity in the months preceding the Düzce earthquake over that area. With such quiet pre-Düzce activity, adjustment of Omori's law and ETAS model is not reliable, thus preventing to run any quantitative analysis of seismicity rate variations after the Düzce earthquake. For the same reason, the dimensions of the selected areas were chosen in order to contain a sufficient number of events for running reliable model parameter inversions, and also to be greater than typical epicentral errors (i.e., a few kilometers).

[16] Thus we distinguish a western region, extending from the epicenter of the Izmit earthquake to the gulf of Izmit, beyond the bay of Yalova, and an eastern region, covering the area from the Izmit earthquake epicenter to the town of Karadere, in order not to include the aftershock activity linked with the rupture of the Düzce fault (Figure 1). We apply the method presented in section 3 to these two areas, covering most of the Izmit earthquake aftershock activity.

### 4.1. Eastern Region

[17] In the area located to the east of the Izmit epicenter (Figure 1), two consecutive changes in seismicity rate are observable.

#### 4.1.1. Pre-Düzce Reactivation

[18] Reactivation of seismicity occurred in the 5 days preceding the Düzce earthquake. As visible on Figure 3a (top), the best fit model clearly underestimates the activity during the interval spanning from day 311 to $T_D = 316.7$

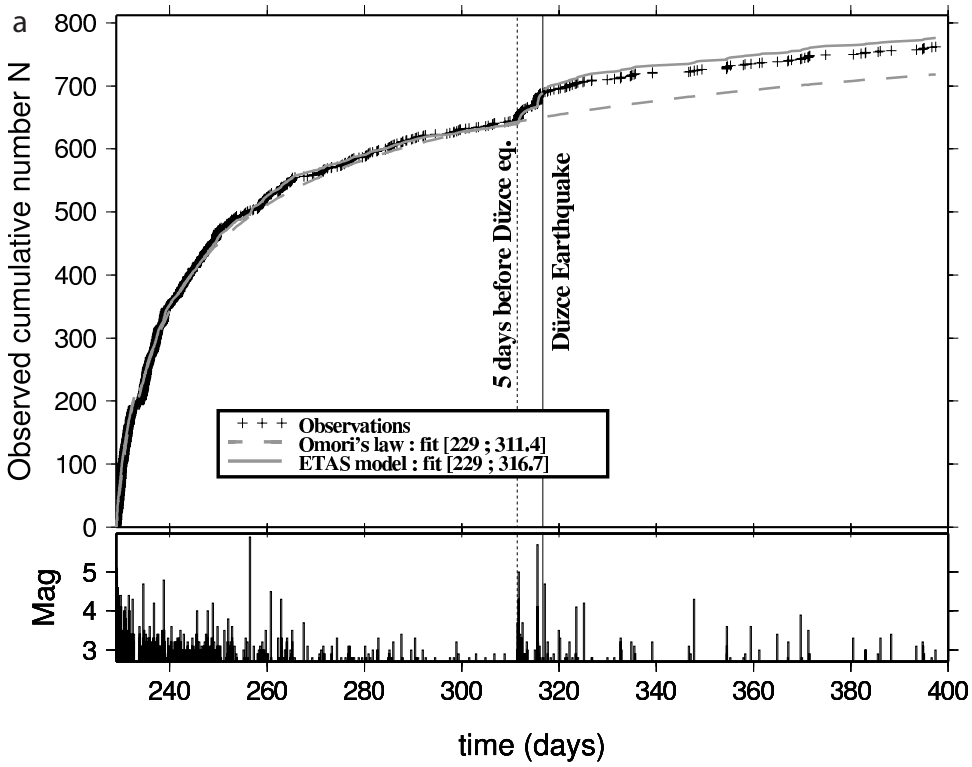


**Figure 3.** Analysis of seismicity rates following the Düzce earthquake. (a) Fault segments located to the east of the Izmit epicenter. (b) Fault segments located to the west of the Izmit epicenter. (c) Yalova area. Time $t$ is expressed in days, Izmit and Düzce earthquakes occurring on days 229 and 316.7, respectively. Origin time is 1 January 1999, 0000 UT. Every plot contains two parts: (top) Comparison of cumulative seismicity rates obtained from Kandilli observatory catalog (crosses) with the best adjusted models (Omori-Utsu's law, ETAS). Grey dashed line indicates Omori-Utsu's law adjustment and extrapolation. Grey line indicates ETAS model fit up to day 316 and its corresponding extrapolation. (bottom) Magnitude of events for this area.

(corresponding to the occurrence of the Düzce earthquake). Extrapolated activity during that target interval is based on the Omori-Utsu's decay law adjusted for the time period spanning from the Izmit earthquake to 5 days before Düzce (i.e., days $T_I = 229$ to 311). The temporal decay of the Izmit earthquake aftershock sequence is very well explained by the Omori-Utsu's law up to day 311. Compared to this model, the rates observed between day 311 to the Düzce earthquake are anomalously high, this departure being quite significant ($\gamma > 6$). Such a reactivation is therefore very unlikely to happen by pure chance if the Izmit aftershock sequence was to decay "normally" in this area. This argues in favor of an activation process not simply deriving from the "normal" decay of the Izmit earthquake aftershock sequence, but more likely attributable to secondary aftershock generation processes. This point is also supported by the very good adjustment of the ETAS model on a temporal interval spanning from the Izmit earthquake to $T_D = 316.7$ (see Figure 3a (top)). This shows that the 5-day-long reactivation can be suitably modeled as an increase in seismicity rate consisting of aftershocks of two $M_w \geq 5$ events occurring 5 days and 1 day before the Düzce earthquake, respectively, the latter event being the $M_w$ 5.7 Sapanca Lake earthquake (40.74°N, 30.24°E; the second largest event of Izmit earthquake aftershock sequence); see Figure 3a (bottom).

[19] This result is in agreement with a study of *Bouchon and Karabulut* [2002], who focused on the anomalously high seismic activity in the 5 hours preceding the Düzce earthquake. Particularly, they reported an active cluster of seismicity in the middle of the Izmit rupture and identified it as aftershock activity following the $M_w$ 5.7 Sapanca Lake earthquake that occurred about 24 hours before the Düzce event. Furthermore, our analysis suggests that the 7 November 1999 (day 311) $M_w$ 5.0 event located near Akyazi (40.74°N, 30.69°E), about 40 km east of the Sapanca Lake earthquake epicenter, also accounted for the early activity of this activation episode. As shown by *Bouchon and Karabulut* [2002], this led to a significantly high seismic activity on the Karadere segment of Izmit rupture, compared to what was expected from a *Reasenberg and Jones* [1989, 1994] aftershock decay rate model. Though both our analysis and Reasenberg and Jones' model are based on the Omori-Utsu decay law, we believe, however, that our method is more reliable in estimating the Izmit aftershock sequence seismicity variations because we obtained the optimal parameter set $\theta^\star$ (including the $p$ value) that best mimics our data.

[20] The observation of anomalously high seismicity rates in the 5 days preceding the Düzce event, in an $\simeq$ 80-km-long area, related to these two $M_w \geq 5$ aftershocks of the Izmit earthquake (Figure 3a, bottom) strongly suggests a

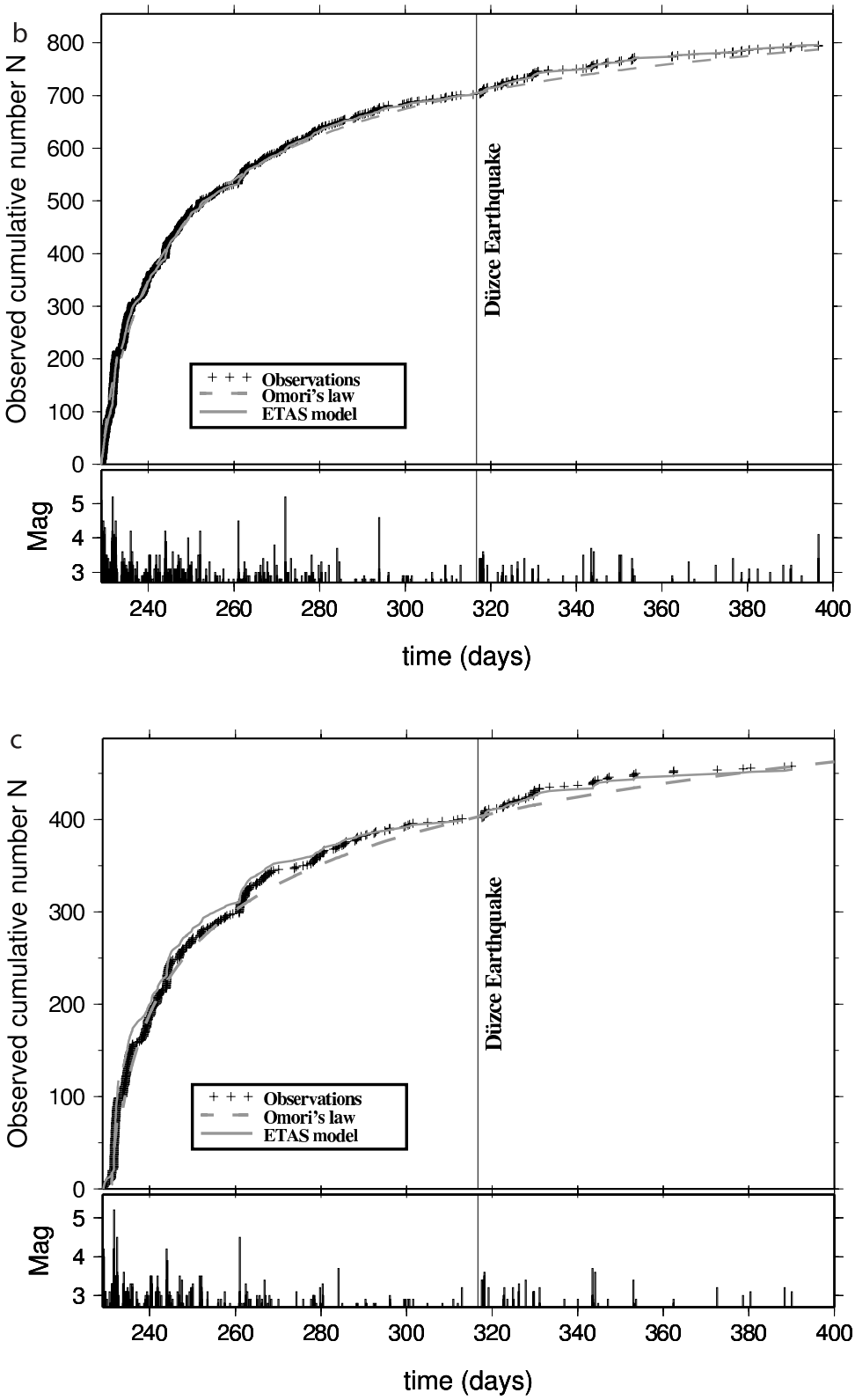


**Figure 3.** (continued)

relationship between these events and the Düzce earthquake, though the nature of it is not identified. In particular, static stresses created by the two $M_w \geq 5$ earthquakes on the Düzce hypocenter are small, the distance being several times the rupture length. A cascade of dynamically triggered events starting from the $M_w$5.7 Sapanca Lake earthquake and eventually leading to the Düzce earthquake would appear more plausible, even though this is pure speculation.

#### 4.1.2. Post-Düzce Quiescence

[21] Extrapolation of the ETAS model to the 3 months following the Düzce earthquake (i.e., up to day 400) suggests that the expected seismicity should be more active

**Table 1.** Recapitulative of Estimated Seismicity Rate Changes[a]

| Area | Fit Interval | Target Interval (TI) | Number of Observations in TI | Number of Extrapolations in TI | $\gamma$ |
|---|---|---|---|---|---|
| | | *Omori-Utsu* | | | |
| East | [229; 311] | [311; 316.7] | 45 | 9.37 | $\rightarrow +\infty$ |
| West | [229; 316.7] | [316.7; 330] | 40 | 19.34 | 4.92 |
| West | [229; 316.7] | [316.7; 350] | 61 | 42.99 | 2.43 |
| West | [229; 316.7] | [316.7; 400] | 93 | 84.95 | 0.75 |
| Yalova | [231; 316.7] | [316.7; 330] | 31 | 12.92 | 5.26 |
| Yalova | [231; 316.7] | [316.7; 350] | 45 | 29.19 | 2.62 |
| Yalova | [231; 316.7] | [316.7; 400] | 57 | 62.59 | −0.58 |
| Yalova | [231; 316.7] | [316.7; 731] | 501 | 549.94 | −1.74 |
| | | *ETAS* | | | |
| East | [229; 316.7] | [316.7; 400] | 73 | 87.28 | −1.17 |
| Yalova | [229; 316.7] | [316.7; 400] | 57 | 53.13 | 0.57 |

[a]We distinguish each area of study and also each model employed to provide the $\gamma$ statistics quantifying the triggering effect.

than is actually observed in this area. We estimate a significance level of $\gamma = -1.17$ (i.e., a 6.8% probability to see this feature happening naturally by chance) that the observed post-Düzce activity rate is smaller than the expected (i.e., modeled) post-Düzce rate, in the first 3 months; see Table 1.

[22] However, this observed quiescence could be a consequence of a temporally higher detection threshold $M_c$ over this region following the Düzce event, as already mentioned in section 2. Such an increase in the magnitude of completeness can either be introduced by a less exhaustive processing of the seismic signals, therefore limiting the catalogue to the strongest Düzce aftershocks, or by a change in the seismological network. The later actually occurred in this region after the Düzce earthquake, as 10 stations were removed from this region and installed closer to the Düzce epicenter area (H. Karabulut, personal communication, 2005).

[23] An increase in $M_c$ cannot be directly tested by the classical method of fitting a Gutenberg-Richter law and searching for a departure at magnitudes smaller than $M_c$, since the observed quiescence only lasts for about 15 days, during which interval 17 earthquakes occurred with magnitudes above the pre-Düzce $M_c$ of 2.7. This number is too low for a reliable estimate of the Gutenberg-Richter law. We therefore adopt a different approach: we estimate the change $\delta M_c$ that would explain this decrease in seismicity rate, and check whether such a change would seem plausible given the loss of 10 local stations. The null hypothesis therefore consists of supposing that the observed post-Düzce seismicity rate can be fully described by the ETAS extrapolated rate $\lambda_0$, along with an increase in the detection threshold $\delta M_c$. We define the probability density function $f(\delta M_c)$ that this $\delta M_c$ can explain the observation of $N = 17$ events above the new detection threshold occurring in the first 15 days from the Düzce earthquake:

$$f(\delta M_c) = \frac{\beta}{N!}\tilde{\lambda_0}^{N+1}\exp\left(-\tilde{\lambda_0}\right) \tag{10}$$

where $\tilde{\lambda_0} = \lambda_0 \times 10^{-b\ \delta Mc}$ with $\lambda_0$ corresponding to the extrapolated ETAS rate of seismicity for the 15 days post-Düzce time period, and $\beta = b\ln 10$ with $b$ being the parameter of the Gutenberg-Richter relation. This PDF (see Figure 4a) suggests that an increase $\delta M_c \sim 0.1-0.15$ is very likely to explain the observed seismicity. This seems a realistic value for the actual $\delta M_c$ caused by the removal of

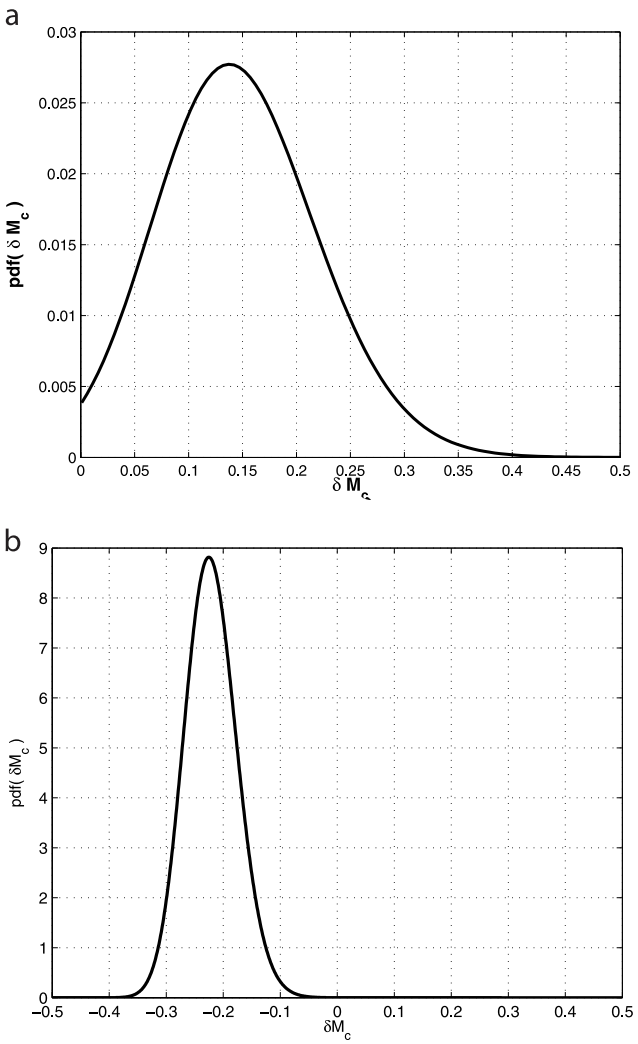


**Figure 4.** Probability density functions that the $N$ observed events in the 15 days after the Düzce earthquake can be explained by an increase in magnitude of completeness $\delta M_c$ for (a) the eastern region and (b) the Yalova area.

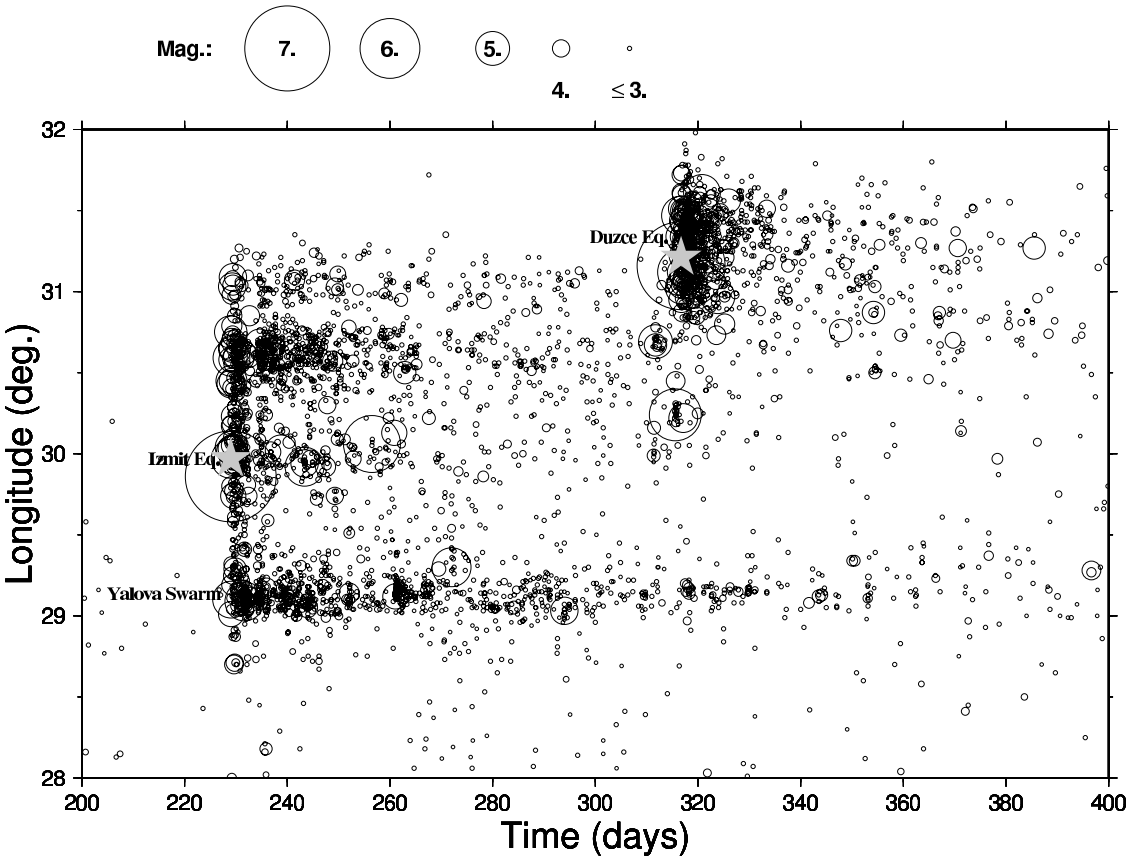


**Figure 5.** Evolution of the seismicity along the western North Anatolian Fault, between longitudes 28°E and 32°E. Aftershock locations are projected onto their longitude coordinate. Time of occurrence is expressed in days (origin time is taken on 1 January 1999 at 0000 UT). Seismic activity linked with the swarm of Yalova presents a strong and long-lasting activation after the Izmit earthquake.

10 stations. The apparent shadow is therefore very likely to be artificial, with an instrumental origin.

### 4.2. Western Region

[24] We now analyze the variation of the seismicity rate over the area located to the west of Izmit epicenter (Figure 1). We adjust the two models on a period ranging from the occurrence of the Izmit earthquake to just before the Düzce earthquake (i.e., days 229 to 316.7), see Figure 3b. Contrary to what is observed in the east, the western area does not show any sign of reactivation preceding the Düzce earthquake. Extrapolation of the best fitted Omori-Utsu's law after the Düzce earthquake shows a clear underestimation of the seismicity rate during that time. For 2 weeks after the Düzce earthquake, the data show a significant ($\gamma$ = 4.92) increase in seismicity rate with respect to the extrapolated Omori-Utsu's law. Such an observation suggests this region experienced a triggering episode consecutive to the Düzce earthquake.

[25] However, extrapolation of this model over a longer time period (i.e., from day 316.7 up to day 350 or 400) shows a decreasing $\gamma$ value when increasing the duration of the extrapolated interval, compare Table 1. This feature argues in favor of a temporally bounded triggering episode. We thus propose that the triggering episode lasted at least 2 weeks to at most 1–2 months over this area, as the $\gamma$ value indicates a much lower significance level after that period.

### 4.3. Yalova Cluster

#### 4.3.1. Measuring Seismic Activation At Yalova

[26] Seismic activity observed to the west of Izmit epicenter includes a cluster located in the vicinity of the town of Yalova (Figure 1). Most of the post-Düzce seismicity in the western region is confined to this area (Figure 5) and after careful examination of the western area seismicity, we could verify that all triggered activity took place within this cluster. Furthermore, this cluster occurred in a very peculiar region with regards to its tectonic and geological settings. Compared to the other NAF segments that ruptured with mostly strike-slip motions during the Izmit earthquake, fault segments along the coasts of the Yalova bay are characterized by normal faulting [*Karabulut et al.*, 2002], associated with a seismicity characterized by high *b* value [*Aktar et al.*, 2004]. Also, the area of Yalova is famous for its geothermal activity, with hot springs located 10 km SW from the city, providing water suitable both for bathing and drinking. Thermal activity in Yalova has been reported since historical times, and the region is now under protection, prohibiting industrial or scientific extraction of its natural resources.

[27] As illustrated in Figure 5, this area underwent a strong and long-lasting activation of seismicity following

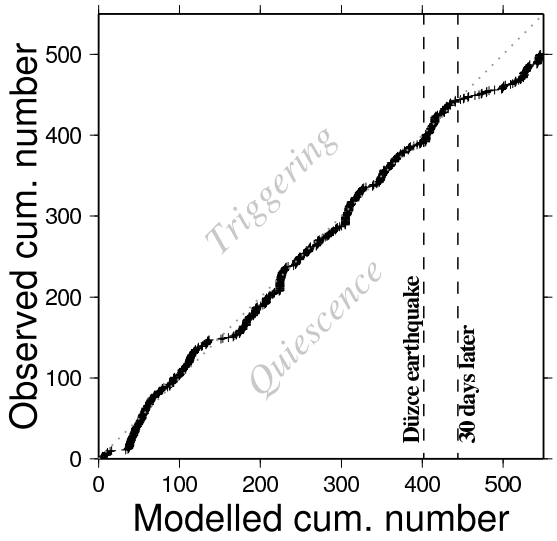


**Figure 6.** Comparison of the observed versus the expected number of aftershocks for Yalova area from Izmit earthquake to the end of year 2000. Modeled number is deduced from the best fitted Omori-Utsu's law. The dotted line signifies a perfect match between modeling and observations. Points located above this line indicate an underestimation of the seismicity by the model, i.e., a triggering episode, whereas points located under this line present an overestimation of the seismicity by the model (quiescence). Note the strong quiescence starting about 30 days after the Düzce earthquake.

the Izmit earthquake. This activity really began 2 days after the main shock [*Özalaybey et al.*, 2002; *Karabulut et al.*, 2002]. The two Omori-Utsu's law and ETAS model were adjusted to the data for a period ranging from Julian day 231 (2 days after the Izmit earthquake) to $T_D$ = 316.7 (time of the Düzce earthquake), see Figure 3c (top). One may notice that models adjustments for this period show poorer fits than for the eastern and western regions. This is a consequence of trying to make the Yalova area as small as possible, thus reducing the number of aftershocks on which seismicity rates are estimated. Consequently, discrepancy between the best fit models and data for the pre-Düzce period should not be interpreted as triggered/quiet episodes, but rather as a measure of the quality of fit of the two models on the data. Analysis of variations in seismicity rates for this cluster shows a clear reactivation of the seismic activity in the 15 days following the Düzce earthquake. Furthermore, early post-Düzce aftershocks magnitudes for this cluster are greater than for aftershocks occurring in the 30 days preceding the Düzce earthquake. This observation is supported by a decrease of Gutenberg-Richter's law *b* value, from the pre-Düzce interval to the post-Düzce interval. For 2 weeks after the Düzce event, this triggering episode lead to $\gamma$ values of 5.26 when compared to an extrapolated Omori-Utsu's law (Figure 3c). Results summarized in Table 1 highlight the strength of this triggering episode, as its effect on $\gamma$ values is still significant in the month following the Düzce earthquake. Recalling the $f(\delta M_c)$ calculation made in section 4.1.2, we find here that the observed post-Düzce activity in this area can be explained by a decrease $\delta M_c \sim -0.2$ of the magnitude of completeness. As there is no reason for such a decrease of the detection threshold (all stations located around Yalova were maintained and none added (H. Karabulut, personal communication, 2005)), this analysis clearly indicates the existence of a triggering episode (Figure 4b). The nature and probable causes of this triggering are discussed in section 4.3.2.

[28] In addition to this post-Düzce triggering episode, analysis of the Düzce aftershock sequence up to the end of year 2000 (day 731) suggests that a quiescence followed that triggering episode, starting about 30 days after the Düzce earthquake. Figure 6 compares the observed and the modeled number of events, the latter according to the best fitted Omori-Utsu's law. This quiescence is found to be significant at the 98.1% level ($\gamma$ value of $-1.73$).

#### 4.3.2. A Case of Dynamic Triggering?

[29] We run an extrapolation of the ETAS model on the post-Düzce seismicity at Yalova. The resulting curve, shown on Figure 3c (top), does not depart significantly from the post-Düzce data in the next 15 days, suggesting that the best fit ETAS model does well in explaining the earthquake occurrences during that time interval. We recall that this model is fit on pre-Düzce data only.

[30] This observation is similar to one made in the eastern region, for the 5 days preceding the Düzce earthquake: the seismic activity significantly departs from the extrapolated Omori-Utsu's activity rate, therefore indicating triggering, but can be well accounted for by the ETAS model if one considers the earthquakes after Düzce as local triggers. Since the ETAS model fits the post-Düzce activity, we interpret this activity to be self-sustained with the same aftershock generation process as was estimated on pre-Düzce activity. As the agreement between ETAS model and observed events starts soon after the Düzce earthquake, we infer that the perturbation seen by the seismogenic process and leading to the triggering of seismicity, was short-lived. We propose that this short-lived character of the perturbation can be associated to transient triggering, caused by the passage of seismic waves generated by the Düzce earthquake, along with the presence of pressurized fluids in this zone.

[31] We model the stress transfer caused by the Düzce earthquake on an hypothetical fault located in the center of the Yalova cluster, with azimuth and dip set to 265° and 70°, respectively (deduced from focal mechanisms presented by *Karabulut et al.* [2002]). For the stress calculations based on the discrete wave number method [*Bouchon*, 1981; *Cotton and Coutant*, 1997], we used the results of the kinematic inversion of the Düzce earthquake presented by *Bouin et al.* [2004], as input parameters for the model. The three projected components of the stress tensor on the target fault plane are represented in Figure 7, for the 100 s following the occurrence of the Düzce earthquake. The arrival of transient waves 50 s. after the main shock produced a maximum dynamic stress load of several bars. Static shear stress produced at Yalova by the Düzce earthquake is very weak, with contribution of about 100 Pa. Moreover, additional water level data support the idea that the Düzce earthquake could be responsible for changes in hydraulic settings at Yalova. No well data are available around Yalova, as

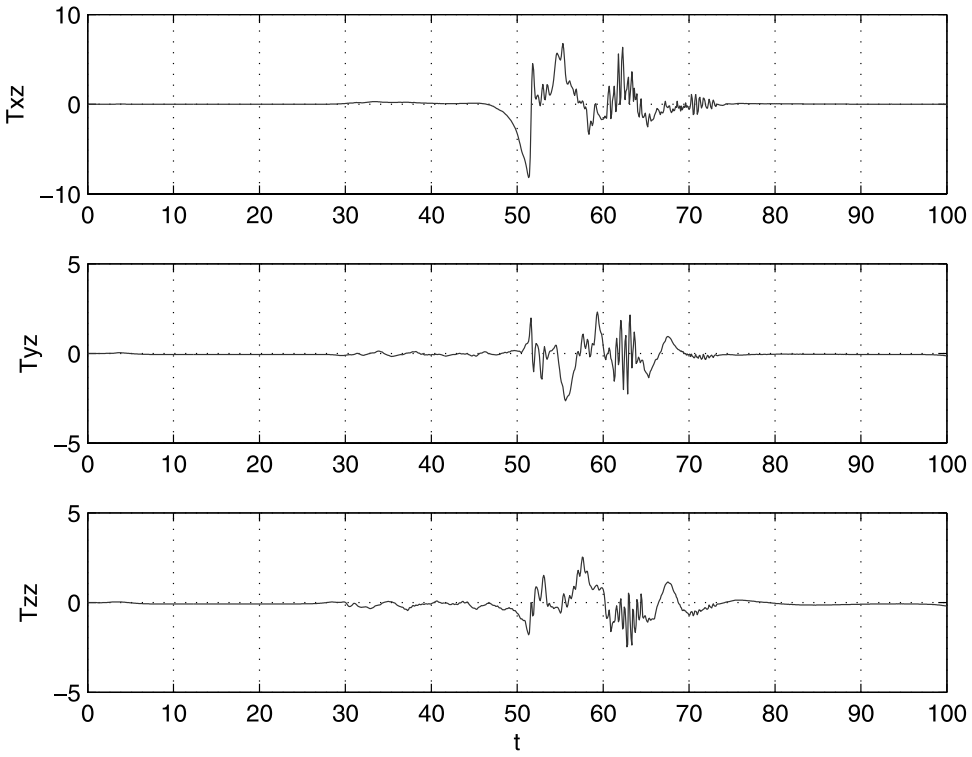


**Figure 7.** Modeling of dynamic stress transfer generated by the Düzce earthquake at the center of the Yalova cluster for the three components of the stress tensor projected onto the target fault plane $T_{xz}$, $T_{yz}$, and $T_{zz}$. The $X$ axis lies in the strike direction, $Y$ axis lies in the updip direction, and the $Z$ axis is normal to the fault plane. Time on the horizontal axis is graduated in seconds; stress is graduated in bars. The target fault plane is located 177 km WSW from the Düzce epicenter with an azimuth of 265° and a dip of 70° [*Karabulut et al.*, 2002]. Although the static component is very low, transient stress can reach up to several bars of loading for each one of the three components. Modeled frequency range lies between 0 and 5 Hz.

drilling is prohibited in this area, according to the will of Atatürk, the founder of Republic of Turkey. However, we obtained water level data from a well located in Armutlu, about 30 km southwest from Yalova (see Figure 1). For this well, *Simsek* [2005] reports a change in water level, which was below the wellhead before 12 November 1999 and then increased to form an artesian flow. In addition, 2 weeks before the Izmit earthquake, measurements at Yalova thermal water springs showed an increase in flow rate with a high deep water content [*Simsek*, 2005]. These are clear signs of deep-seated earthquake-related changes that might affect failure at seismogenic depths.

[32] As mentioned in section 4.3.1, seismicity in Yalova experienced triggering followed by quiescence. In a previous numerical study, *Gomberg et al.* [1998] found that for a transient load over a population of faults controlled by rate-and-state friction, the seismic activity would increase for a duration comparable to the duration of the transient load. A quiescent period would then follow this activation. Here, we infer that the transient perturbation generated secondary aftershocks, indicated by the goodness of fit of the ETAS model during that period, that may have amplified and lengthened the seismic response of this cluster, leading to an activation duration greater than expected for cases of dynamic triggering [*Gomberg et al.*, 1998; *Belardinelli et al.*, 2003]. However, we point out here an observed quiescence after the triggering episode, that these models would present as an expected consequence of the dynamic triggering process.

[33] Another striking feature of this reactivation episode is that the seismic activity of the cluster restarted after a time delay of about 18 hours following the Düzce earthquake. In most studies, dynamically triggered seismic activity starts in the first seconds to minutes following the arrival of *P* waves [*Brodsky and Prejean*, 2005; *Husen et al.*, 2004; *West et al.*, 2005] and is often correlated with the high-amplitude surface wave arrivals [*Hill et al.*, 1993; *Brodsky et al.*, 2000; *Prejean et al.*, 2004; *West et al.*, 2005]. However, *Hill et al.* [1993] reported activity starting 19, 23, and 33 hours after the 1992 Landers earthquake *P* wave arrivals at Mono Basin, at Burney, California, and in Cascade, Idaho, respectively. They also pointed out the increasing difficulty to associate any delayed aftershock reactivation with increasing delays from the main shock. Though this does not presume on the physical potentiality for a delayed triggering mechanism, it rather highlights the difficulty of linking effects and causes when long delays separate them. *Prejean et al.* [2004] also detected a cluster of activity with a maximum magnitude of 3.0 starting in Long Valley

Caldera, California, more than 23 hours following the arrival of the 2002 Denali Fault earthquake wave train and lasting for 17 days. The reactivation in Yalova after the Düzce earthquake is very similar to the behavior of this cluster. Also, a cluster of seismicity started in Nicobar Islands about 30 days following the great 2004 $M_w$ 9.0 Sumatra earthquake. This raises questions about the existence of an upper temporal limit for delayed triggered activity following a main shock. A recent study by *Parsons* [2005] suggests that delayed dynamic triggering can occur if passing waves can affect the mean critical slip distance $D_c$ of fault driven by rate-and-state friction laws. However, while providing a framework for explaining Omori-like decays of purely dynamically triggered activity, this model cannot explain the lack of seismicity observed for the first 18 hours.

[34] Plausible mechanisms responsible for those delays probably require nonlinear processes. We thus suggest that the observed 18-hour delay at Yalova could result from a complex interaction between geothermal fluids circulation, repeated transient deformation episodes, extensional tectonic settings and the heavily fractured state of this area [*Aktar et al.*, 2004]. In particular, this 18-hour delay is very similar to the 48-hour delay characterizing the activation at Yalova following the Izmit earthquake [*Özalaybey et al.*, 2002], making such a delay a property inherent to the geological setting of this area.

## 5. Conclusion

[35] We have presented an analysis of the seismicity rate changes along the Izmit-ruptured segments of the North Anatolian Fault caused by the Düzce earthquake. Seismicity rates were adjusted by an Omori-Utsu's law or by an ETAS model to the Izmit earthquake aftershock sequence up to the occurrence time of the Düzce main shock, 3 months later. We studied the statistical significance of the departure of the observed seismicity rate following the Düzce earthquake from what could be expected if this earthquake had not occurred, in order to detect episodes of triggering or quiescence.

[36] For reliability of the estimated rate, we focused on two regions so that each contains a sufficient number of aftershocks for the inversion procedure and covers an area greater than the typical error on aftershock location. Consequently, we separately analyzed an eastern and a western part of the Izmit fault zone.

[37] The eastern part of the Izmit rupture shows an anomalous reactivation of seismicity in the 5 days preceding the Düzce earthquake, that we infer to be linked with the occurrence of two $M_w \geq 5$ aftershocks of the Izmit earthquake. Moreover, post-Düzce seismicity in this region experienced quiescence as suggested by comparison of the observed data with the extrapolation of the best fit ETAS model. However, this quiescence is likely to be spurious, as it coincides with a redeployment of the seismological network further east, and could be fully explained by considering a slight increase ($\delta M_c$ = 0.1 to 0.15) of the detection threshold $M_c$.

[38] The western part of the Izmit rupture shows a significant reactivation following the Düzce earthquake. As most aftershocks occurring in this region after the Düzce earthquake clustered in the vicinity of the geothermal area of Yalova, we isolated the seismicity behavior of this cluster. This area exhibits a significant triggering episode starting 18 hours after the Düzce earthquake. Moreover, we show that this reactivation lasted about 30 days, and was followed by a quiescence. Noticing that such a change is unlikely to be caused by static stress, we argue that this would correspond to a case of delayed dynamic triggering of seismicity by transient waves emitted during the Düzce earthquake. The Yalova cluster experienced a significant quiescence following this triggering episode, that started about 30 days after the Düzce earthquake and lasted for several months. The onset of this quiescence does not coincide with any remarkable seismic event in the vicinity, and could therefore be of aseismic origins.

[39] The seismic behavior observed at Yalova recalls previous reports of dynamic triggering recorded elsewhere in geothermal areas [*Hill et al.*, 1993; *Husen et al.*, 2004; *Husker and Brodsky*, 2004; *Prejean et al.*, 2004]. Pressurized fluids circulation and the highly fractured state of the area are likely to have played an important role in driving its seismic response. We could not however suggest a mechanism to explain the 18-hour delay. This type of delay is probably a characteristic of this area, as triggering was also delayed by about 2 days following the Izmit earthquake. Geothermal areas are very unstable regions, with a fault system in a mechanical equilibrium state very close to the rupture, as suggested by their high sensitivity to transient stress perturbations. By carefully describing the seismic behavior at Yalova, we hope this study may help improving our knowledge on the peculiar seismic response of geothermal areas.

## Appendix A: Mean-Field Extrapolation of the ETAS Model

[40] As invoked in section 3, in some cases, an increase in seismicity rate can be very well accounted for by a standard ETAS model extrapolation [*Ogata*, 1992, 1999, 2005], provided the observed rate and magnitude of events in the extrapolation interval match the magnitude-dependent aftershock production rate predicted by the adjusted ETAS model. Consequently, this type of extrapolation may not discriminate an anomalous reactivation episode under such conditions. This reason led us to introduce the mean-field extrapolation as a more suitable method to detect unexpected behaviors.

[41] As described in equation (3), estimating the seismicity rate at $t$ from the ETAS model requires including all $m_i > m_c$ seismic events occurring at $t_i < t$. Nevertheless, as we want to extrapolate the post-Düzce seismicity rate with no a priori knowledge on the upcoming seismicity, we must at least give the model an estimation of what average activity would be expected. We thus included in the mean-field extrapolation all $m_i \geq m_c$ seismic events occurring at $t < T_D$, in addition to information about the expected magnitudes of upcoming events (for $t \geq T_D$). This last point is based on the estimated $b$ value of the Gutenberg-Richter's law, and information on the expected mean rate of earthquake occurrence is estimated via the branching rate (or average

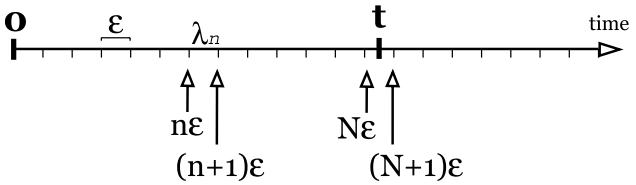


**Figure A1.** Discretization scheme of the time axis.

number of triggers generated by each aftershock, forced to be less than 1, for convergence of the estimate) given by

$$\frac{\beta K_0 c^{1-p}}{(p-1)(\beta-\alpha)} < 1 \tag{A1}$$

where $\beta = b\log(10)$.

## A1. Theory

[42] We here present ways of running a mean-field extrapolation of the ETAS model [*Ogata*, 1992] once the optimal parameter set $\theta = \{K_0; \alpha; c; p\}$ is obtained from an inversion procedure. Note that all event magnitude values $m_i$ are subtracted from the completeness threshold $m_c$. Expression for the extrapolated rate $\lambda_0(t)$ depends on the data set content:

[43] 1. Given $\{t_i; m_i\}$, the occurrence times and magnitudes of the events on a time interval subsequent to the fit interval, one may deduce the mean-field rate $\lambda_0(t)$ as

$$\lambda_0(t) = \int_0^\infty dm \int_{-\infty}^\infty ds\ g(t-s,m)\phi(s,m) \tag{A2}$$

with (1) $[\phi(s, m)] = \Sigma_i \delta(s - t_i)\ \delta(m - m_i)$, (2) $[g(t, m)] = 0$ for $t < 0$, and (3) $[g(t, m)] = K_0\ e^{\alpha m}\ (t + c)^{-p}$ for $t \geq 0$.

[44] 2. Given $\{t_i\}$ but no information on the corresponding $\{m_i\}$, we get

$$\lambda_0(t) = \int_{-\infty}^t ds\ K_0(t-s+c)^{-p}\phi(s) \int_0^\infty dm\ e^{\alpha m} f(m) \tag{A3}$$

where $f(m)$ stands for the probability density function that the magnitude is $m$, according to Gutenberg-Richter's law:

$$f(m) = \beta e^{-\beta m}$$

Thus

$$\lambda_0(t) = \int_{-\infty}^t ds \frac{K_0\beta}{\beta-\alpha}(t-s+c)^{-p}\phi(s) \tag{A4}$$

[45] 3. Neither information on $\{t_i\}$, nor on $\{m_i\}$, but knowing the probability $\lambda(t, t + \varepsilon)$ for an earthquake to occur at time $t_i \in [t; t + \varepsilon]$.

[46] The time axis is thus discretized into equal-sized segments of length $\varepsilon$ (see Figure A1).

[47] Probability density function for a single event to occur in the time interval $[t; t + \varepsilon]$ is given by $(\lambda(t, t + \varepsilon))/\varepsilon$ (with $\varepsilon \ll 1$), then

$$\lambda_0(t) = \int_{-\infty}^t ds \frac{K_0\beta}{\beta-\alpha}(t-s+c)^{-p} \sum_n \frac{\lambda_n(s)}{\varepsilon}$$

where (1) $[n] \geq 0$, (2) $[\lambda_n(s)] = 0$ for $s \notin [n\varepsilon; (n + 1)\varepsilon]$, and (3) $[\lambda_n(s)] = \lambda_n$ for $s \in [n\varepsilon; (n + 1)\varepsilon]$.

[48] Thus

$$\lambda_0(t) = \frac{K_0\beta}{\varepsilon(\beta-\alpha)} \sum_n \lambda_n \int_{\min[n\varepsilon,t]}^{\min[(n+1)\varepsilon,t]} ds(t-s+c)^{-p}$$

from what we get

$$\begin{aligned}\lambda_0(t) = {} & \frac{K_0\beta}{\varepsilon(\beta-\alpha)(1-p)} \sum_{n;(n+1)\varepsilon<t} \lambda_n \\ & \cdot \left([t+c-n\varepsilon]^{1-p} - [t+c-(n+1)\varepsilon]^{1-p}\right) \\ & + \frac{K_0\beta}{\varepsilon(\beta-\alpha)(1-p)} \lambda_N \left([t+c-N\varepsilon]^{1-p} - c^{1-p}\right)\end{aligned} \tag{A5}$$

with $N\varepsilon < t < (N + 1)\ \varepsilon$.

[49] As we discretized the time axis, calculating the mean rate $\lambda_m$ between time indexes $m\varepsilon$ and $(m + 1)\varepsilon$ requires an integration:

$$\lambda_m = \int_{m\varepsilon}^{(m+1)\varepsilon} dt \lambda_0(t)$$

leading to

$$\begin{aligned}\lambda_m = {} & \frac{K_0\beta}{\varepsilon(\beta-\alpha)(1-p)} \sum_{n<m} \lambda_n \\ & \cdot \int_{m\varepsilon}^{(m+1)\varepsilon} dt \left([t+c-n\varepsilon]^{1-p} - [t+c-(n+1)\varepsilon]^{1-p}\right) \\ & + \frac{K_0\beta}{\varepsilon(\beta-\alpha)(1-p)} \lambda_m \int_{m\varepsilon}^{(m+1)\varepsilon} dt \left([t+c-m\varepsilon]^{1-p} - c^{1-p}\right)\end{aligned} \tag{A6}$$

Finally,

$$\lambda_m = \sum_{n\leq m} G_{m-n}\lambda_n \tag{A7}$$

with

$$[G_0] = -\frac{K_0\beta}{\varepsilon(\beta-\alpha)(1-p)} \left[c^{1-p}\varepsilon + \frac{c^{2-p} - (\varepsilon+c)^{2-p}}{2-p}\right]$$

and

$$\begin{aligned}[G_p] = {} & \frac{K_0\beta}{\varepsilon(\beta-\alpha)(1-p)(2-p)} \left[-2(p\varepsilon+c)^{2-p}\right. \\ & \left. + ((p-1)\varepsilon+c)^{2-p} + ((p+1)\varepsilon+c)^{2-p}\right] (p > 0).\end{aligned}$$

[50] Calculation of the mean-field rate is then performed as follows:

[51] 1. Calculation of the source term $\lambda^{(0)}$. In our case, this term is calculated from the known series of seismicity up to the end of the fit interval.

[52] 2. Calculation of $G$.

[53] 3. Iterations up to $i \sim 100$: $\lambda^{(i+1)} = G\lambda^{(i)}$. One should verify that the iteration process does converge toward 0, which is guaranteed for branching rate value $(\beta K_0 c^{1-p})/[(p - 1)\ (\beta - \alpha)] < 1$. The furthest the branching rate to 1, the fastest the convergence toward 0.

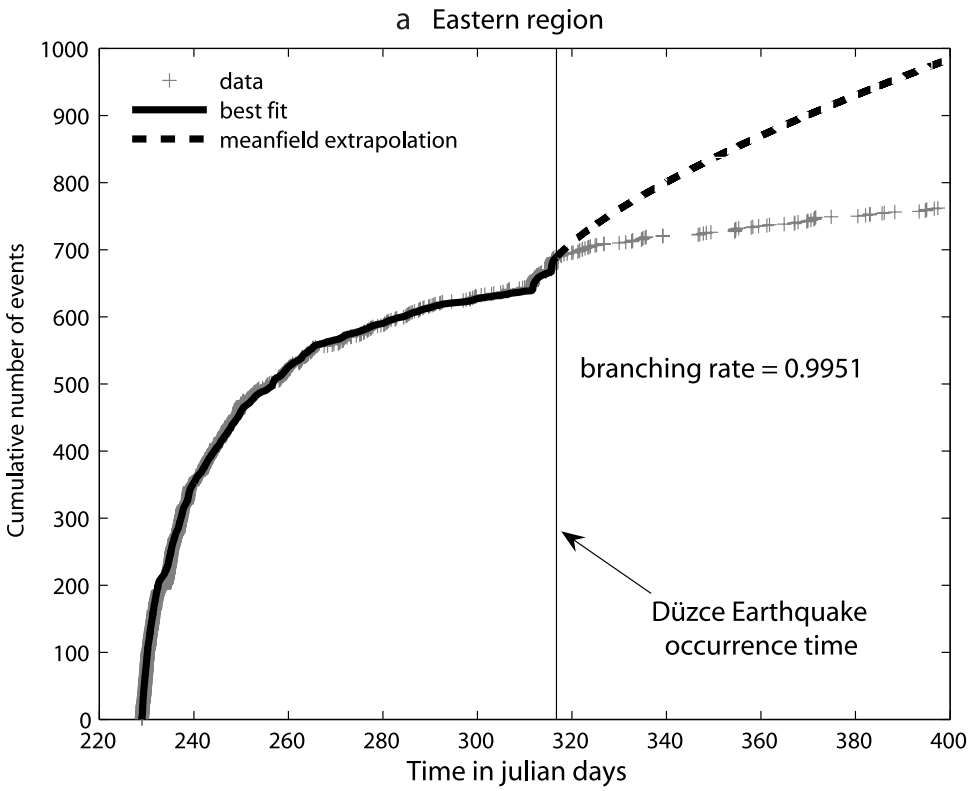


**Figure A2.** Best fit and mean-field extrapolation of the ETAS model on three data sets used in this study: (a) the eastern region (b) the western region, and (c) the Yalova area.

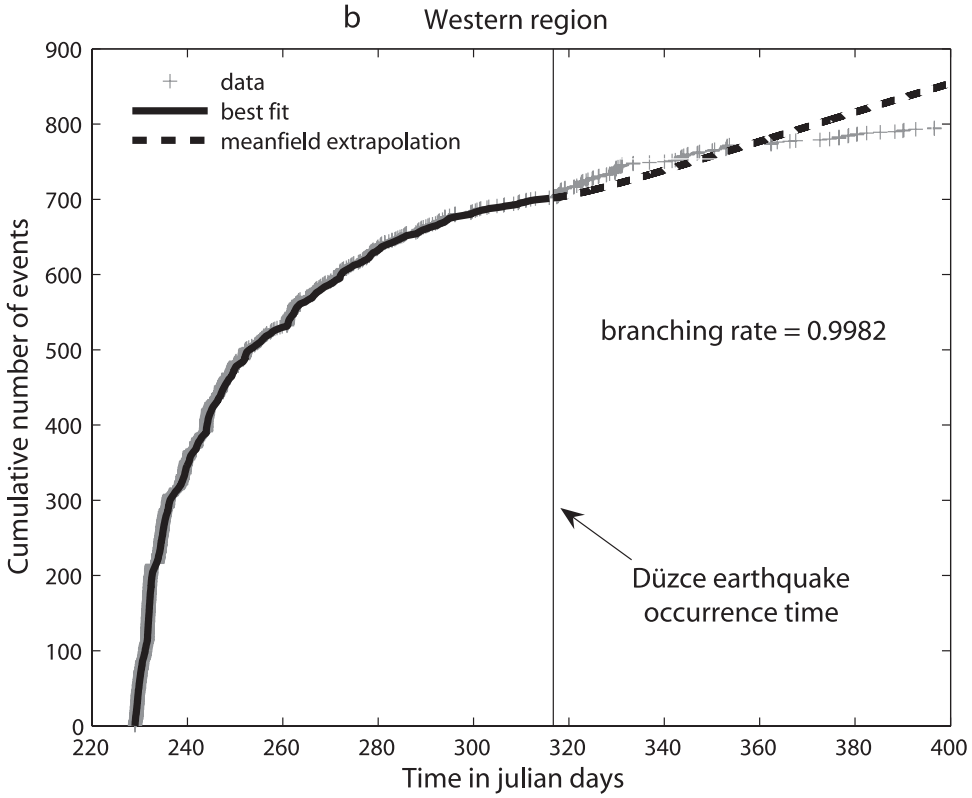


**Figure A2.** (continued)

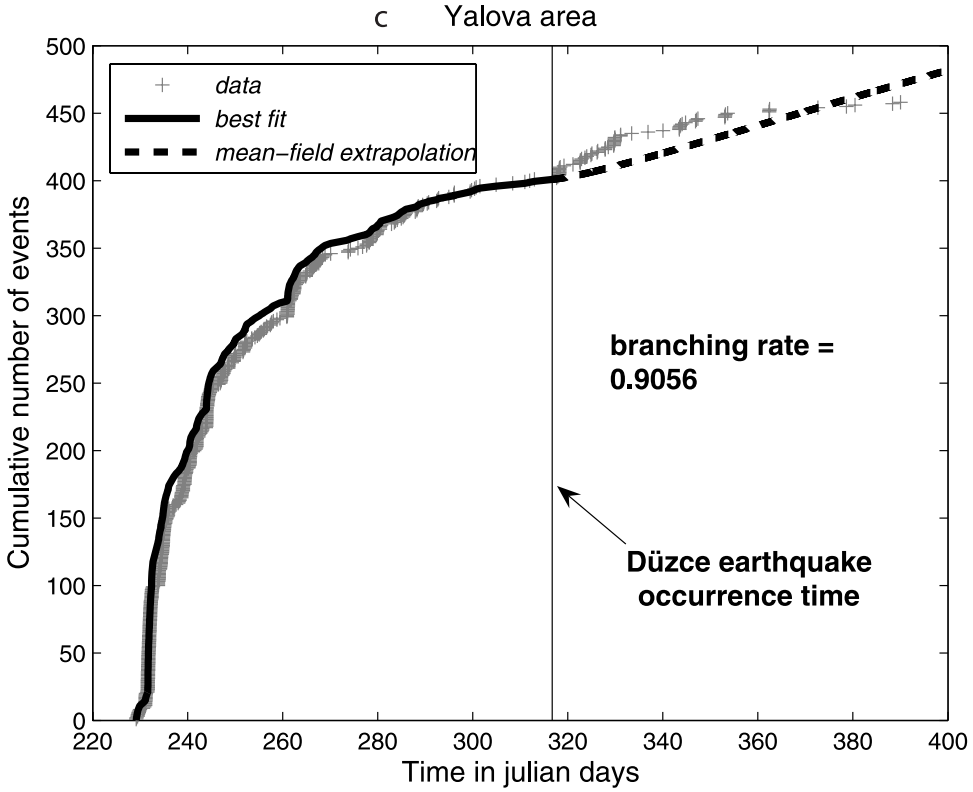


**Figure A2.** (continued)

[54] 4. Summation: $\Lambda = \lambda^{(0)} + \lambda^{(1)} + \ldots + \lambda^{(i)} + \ldots$ in order to obtain the mean-field rate $\Lambda$.

[55] To conclude, we would like to emphasize the fact that the extrapolated seismicity rate should be understood as a realization of a stochastic process, and that consequently, its distribution can be obtained by running Monte Carlo analysis. However, such a procedure is somewhat tedious and time consuming for any standard PC. So we opted for a mean-field extrapolation procedure that, although it gives no information on the extrapolated rate distribution, provides an estimation of the seismicity rate ensemble average that can expected.

### A2. Examples

[56] We performed this mean-field extrapolation on the data set described in this study. Figures A2a, A2b, and A2c show ETAS mean-field extrapolated rates for the eastern region, the western region, and the Yalova area, respectively. As it is visible on these plots, mean-field extrapolated activity is exploding (i.e., tends toward an infinite number of expected events). This problematic behavior is a consequence of a branching rate value very close to 1, as systematically returned by the inversion procedure. Consequently, we preferred not to include these exploding extrapolations into the results presented in this study because discussions based on unrealistic predictions may weaken our conclusions.

[57] **Acknowledgments.** We are very grateful to scientists from the Kandilli Observatory and Earthquake Research Institute at Istanbul and especially to Hayrullah Karabulut and Mustafa Aktar for the data they kindly provided to us and for their help in our attempt to extract the most possible information from the catalogues. We are also grateful to Serdar Özalaybey for providing data from the TÜBITAK Marmara Research Center. We also acknowledge Joan Gomberg, Tom Parsons, and an anonymous reviewer for their constructive comments which helped in significantly improving the manuscript.

## References

Aktar, M., S. Özalaybey, M. Ergin, H. Karabulut, M.-P. Bouin, C. Tapirdamaz, F. Biçmen, A. Yörük, and M. Bouchon (2004), Spatial variation of aftershock activity across the rupture zone of the 17 August 1999 Izmit earthquake, Turkey, *Tectonophysics*, *391*, 325–334.

Belardinelli, M. E., A. Bizzarri, and M. Cocco (2003), Earthquake triggering by static and dynamic stress changes, *J. Geophys. Res.*, *108*(B3), 2135, doi:10.1029/2002JB001779.

Bouchon, M. (1981), A simple method to calculate Green's functions in elastic layered media, *Bull. Seismol. Soc. Am.*, *71*, 959–971.

Bouchon, M., and H. Karabulut (2002), A note on seismic activity near the eastern termination of the Izmit rupture in the hours preceding the Duzce earthquake, *Bull. Seismol. Soc. Am.*, *92*, 406–410.

Bouin, M.-P., M. Bouchon, H. Karabulut, and M. Aktar (2004), Rupture process of the 1999 November 12 Düzce (Turkey) earthquake deduced from strong motion and Global Positioning System measurements, *Geophys. J. Int.*, *159*, 207–211.

Brodsky, E. E., and S. G. Prejean (2005), New constraints on mechanisms of remotely triggered seismicity at Long Valley Caldera, *J. Geophys. Res.*, *110*, B04302, doi:10.1029/2004JB003211.

Brodsky, E. E., V. Karakostas, and H. Kanamori (2000), A new observation of dynamically triggered regional seismicity: earthquakes in Greece following the August, 1999, Izmit, Turkey earthquake, *Geophys. Res. Lett.*, *27*, 2741–2744.

Bürgmann, R., S. Ergintav, P. Segall, E. H. Hearn, S. McClusky, R. E. Reilinger, H. Woith, and J. Zschau (2002), Time-dependent distributed afterslip on and deep below the Izmit earthquake rupture, *Bull. Seismol. Soc. Am.*, *92*, 126–137.

Cotton, F., and O. Coutant (1997), Dynamic stress variations due to shear faults in a plane-layered medium, *Geophys. J. Int.*, *128*, 676–688.

Felzer, K. R., and E. E. Brodsky (2005), Testing the stress shadow hypothesis, *J. Geophys. Res.*, *110*, B05S09, doi:10.1029/2004JB003277.

Gomberg, J., N. M. Beeler, M. L. Blanpied, and P. Bodin (1998), Earthquake triggering by transient and static deformations, *J. Geophys. Res.*, *103*(B10), 24,411–24,426.

Gomberg, J., P. A. Reasenberg, P. Bodin, and R. A. Harris (2001), Earthquake triggering by seismic waves following the Landers and Hector Mine earthquakes, *Nature*, *411*, 462–466.

Gomberg, J., P. Bodin, K. Larson, and H. Dragert (2004), Earthquakes nucleated by transient deformations caused by the $M = 7.9$ Denali, Alaska, earthquake, *Nature*, *427*, 621–624.

Hearn, E. H., R. Bürgmann, and R. E. Reilinger (2002), Dynamics of Izmit earthquake postseismic deformation and loading of the Düzce earthquake hypocentre, *Bull. Seismol. Soc. Am.*, *92*, 172–193.

Hill, D. P., P. A. Reasenberg, A. Michael, and W. J. Arabaz (1993), Seismicity remotely triggered by the $M_w$7.3 Landers, california, earthquake, *Science*, *260*, 1617–1623.

Husen, S., S. Wiemer, and R. B. Smith (2004), Remotely triggered seismicity in the Yellowstone National Park region by the 2002 $M_w$ 7.9 Denali Fault earthquake, Alaska, *Bull. Seismol. Soc. Am.*, *94*, S317–S331.

Husker, A. L., and E. E. Brodsky (2004), Seismicity in Idaho and Montana triggered by the Denali Fault earthquake: A window into the geologic context for seismic triggering, *Bull. Seismol. Soc. Am.*, *94*, S310–S316.

Karabulut, H., M. P. Bouin, M. Bouchon, M. Dietrich, C. Cornou, and M. Aktar (2002), The seismicity in the eastern Marmara Sea after the 17 august 1999 Izmit earthquake, *Bull. Seismol. Soc. Am.*, *92*, 387–393.

Kilb, D., J. Gomberg, and P. Bodin (2000), Triggering of earthquake aftershocks by dynamic stresses, *Nature*, *408*, 570–574.

King, G. C. P., R. S. Stein, and J. Lin (1994), Static stress changes and the triggering of earthquakes, *Bull. Seismol. Soc. Am.*, *84*, 935–953.

King, G. C. P., A. Hubert-Ferrari, S. S. Nalbant, B. Meyer, R. Armijo, and D. Bowman (2001), Coulomb stress interactions and the 17 August 1999 Izmit, Turkey earthquake, *C. R. Acad. Sci.*, *333*, 557–570.

Ma, K., C. Chan, and R. S. Stein (2005), Response of seismicity to Coulomb stress triggers and shadows of the 1999 $M_w = 7.6$ Chi-Chi, Taiwan, earthquake, *J. Geophys. Res.*, *110*, B05S19, doi:10.1029/2004JB003389.

Marsan, D. (2003), Triggering of seismicity at short timescales following Californian earthquakes, *J. Geophys. Res.*, *108*(B5), 2266, doi:10.1029/2002JB001946.

Marsan, D., and S. S. Nalbant (2005), Methods for measuring rate changes: A review and a study of how the $M_w$7.3 Landers earthquake affected the aftershock sequence of the $M_w$6.1 Joshua Tree earthquake, *Pure Appl. Geophys.*, *162*, 1151–1185.

Nalbant, S. S., A. Hubert, and G. C. P. King (1998), Stress coupling between earthquakes in northwest Turkey and the north Aegean Sea, *J. Geophys. Res.*, *103*, 24,469–24,486.

Ogata, Y. (1992), Detection of precursory relative quiescence before great earthquakes through a statistical model, *J. Geophys. Res.*, *97*, 19,845–19,871.

Ogata, Y. (1999), Seismicity analysis through point-process modeling: A review, *Pure Appl. Geophys.*, *155*, 471–507.

Ogata, Y. (2005), Detection of anomalous seismicity as a stress change sensor, *J. Geophys. Res.*, *110*, B05S06, doi:10.1029/2004JB003245.

Özalaybey, S., M. Ergin, M. Aktar, C. Tapirdamaz, F. Biçmen, and A. Yöruk (2002), The 1999 Izmit earthquake sequence in Turkey: Seismological and tectonic aspects, *Bull. Seismol. Soc. Am.*, *92*, 376–386.

Parsons, T. (2005), A hypothesis for delayed dynamic earthquake triggering, *Geophys. Res. Lett.*, *32*, L04302, doi:10.1029/2004GL021811.

Parsons, T., S. Toda, R. S. Stein, A. Barka, and J. H. Dieterich (2000), Heightened odds of large earthquakes near Istanbul: An interaction-based probability calculation, *Science*, *288*, 661–665.

Prejean, S. G., D. P. Hill, E. E. Brodsky, S. E. Hough, M. J. S. Johnson, S. D. Malone, D. H. Oppenheimer, A. M. Pitt, and K. B. Richards-Dinger (2004), Remotely triggered activity on the United States west coast following the $M_w$ 7.9 Denali Fault earthquake, *Bull. Seismol. Soc. Am.*, *94*, S348–S359.

Reasenberg, P. A., and L. M. Jones (1989), Earthquake hazard after a mainshock in California, *Science*, *243*, 1173–1176.

Reasenberg, P. A., and L. M. Jones (1994), Earthquakes aftershocks: Update, *Science*, *265*, 1251–1252.

Simsek, S. (2005), Geothermal activity at earthquake zones and using of geothermal energy on earthquakes areas, in *Geothermal Geochemistry and Some New Geothermal Approaches*, pp. 167–180, Turkish Geotherm. Assoc., Dokuz Eylul Univ., Izmir, Turkey.

Stein, R. S., G. C. P. King, and J. Lin (1992), Change in failure stress on the southern San Andreas fault system caused by the 1992 $M_w = 7.4$ Landers earthquake, *Science*, *258*, 1328–1332.

Toda, S., and R. Stein (2003), Toggling of seismicity by the 1997 Kagoshima earthquake couplet: A demonstration of time-dependent stress transfer, *J. Geophys. Res.*, *108*(B12), 2567, doi:10.1029/2003JB002527.

Utkucu, M., S. S. Nalbant, J. McCloskey, S. Steacy, and O. Alptekin (2003), Slip distribution and stress changes associated with the 1999 November 12, Duzce (Turkey) earthquake ($M_w = 7.1$), *Geophys. J. Int.*, *153*, 229–241.

Utsu, T. (1961), A statistical study on the occurrence of aftershocks, *Geophys. Mag.*, *30*(4), 521–605.

West, M., J. J. Sánchez, and S. R. McNutt (2005), Periodically triggered seismicity at Mount Wrangell, Alaska, after the Sumatra earthquake, *Science*, *308*, 1144–1146.

Woessner, J., E. Hauksson, S. Wiemer, and S. Neukomm (2004), The 1997 Kagoshima (Japan) earthquake doublet: A quantitative analysis of aftershock rate changes, *Geophys. Res. Lett.*, *31*, L03605, doi:10.1029/2003GL018858.

M. Bouchon and G. Daniel, Laboratoire de Géophysique Interne et de Tectonophysique, Université Joseph Fourier, F-38000 Grenoble, France. (guillaume.daniel@obs.ujf-grenoble.fr)

D. Marsan, Laboratoire de Géophysique Interne et Tectonophysique, Université de Savoie, Campus Scientifique, F-73376 Le Bourget du Lac cedex, France.